Available online at www.sciencedirect.com
SCIENCE DIRECT®
Journal of Power Sources 118 (2003) 248–255
JOURNAL OF POWER SOURCES
www.elsevier.com/locate/jpowsour

Performance of a direct methanol fuel cell operated at atmospheric pressure

Nobuyoshi Nakagawa*, Yikun Xiu

Department of Biological and Chemical Engineering, Gunma University, 1-5-1 Tenjincho, Kiryu, Gunma 376-8515, Japan

Abstract

As a fundamental study of the electrode performance of a direct methanol fuel cell (DMFC), DMFCs with different loadings of anode catalyst were prepared and operated with liquid methanol under various conditions at atmospheric pressure. The DMFC employed Nafion 112 as a solid polymer electrolyte and Pt-Ru/C and Pt/C catalysts for the anode and cathode, respectively. The effects of the Pt-Ru loading for anode and, using the cell with an optimum Pt-Ru loading, the temperature and feed rates of the oxidant gas on the cell performance were investigated. The cell performance was analyzed based on the measurement of the current–voltage characteristics and electrode impedance. The performance increased with the increasing Pt-Ru loading up to a certain amount. Over this value, the current density at a low cell voltage decreased with its increase resulting in the reduction of the power density. An unstable and temporal decline in the performance was observed near the vaporization temperature of the feeding liquid and at low feed rate of oxidant gas. It was considered that the mass transfer of the materials related to the electrode reaction was limiting at these conditions. The relatively large power density of 0.12 W/cm^2 was obtained with the optimum Pt-Ru loadings at 363 K under atmospheric pressure.
© 2003 Elsevier Science B.V. All rights reserved.

Keywords: Direct methanol fuel cell; Atmospheric pressure; Electrode impedance; Current–voltage characteristics; Catalyst loading

1. Introduction

Direct methanol fuel cells (DMFCs) are receiving a great deal of attention as alternative power sources especially for automobiles and portable electronic devices. This is due to their positive characteristics such as simple system–structure, reduced system size, weight, high power–generation efficiency and environmental compatibility. The status of the research and development of DMFC including its history has been summarized elsewhere [1]. Recent reports demonstrated a relatively high performance using a solid polymer electrolyte such as Nafion with Pt–Ru alloys as the anode catalyst [2–6] although the problem due to methanol crossover [7–11] still remained. High-pressure operation between 1.5 and 5 atm was chosen to achieve a high performance in the past studies [2,6,12,13], however, some reports [4] suggested a high performance even at atmospheric pressure by optimizing the structures and compositions of the electrodes. Less severe conditions of pressure and temperature for DMFC are favorable especially for portable use.

To optimize the electrode structure, there are many parameters, like the composition of the catalyst itself, catalyst loading, ionomer content in the catalyst layer, porosity of the electrode, etc., that should be evaluated. However, very few reports are available for the effect of such parameters [4,14,15] on the performance of the DMFC. Concerning the relationship between the operating conditions and cell performance, some reports are available [7,12,14]. However, they are not detailed enough to discuss the mechanism related to its performance because it is also affected by the geometry of the flow channels of the liquid and gas [14,16,17] that were different in each study. Impedance studies of the DMFC [18,19] are still lacking and most of the former performance analyses were mainly based on only the direct-current response.

In this study, the effect of catalyst loading of the anode on the performance of the DMFC was investigated in order to optimize the catalyst layer. The performance was evaluated and analyzed by measuring the current–voltage characteristics and electrode impedance at atmospheric pressure. Also, the effects of the operating conditions, i.e. temperature and feed condition of the oxidant gas, were measured using a cell with an optimum catalyst loading.

* Corresponding author. Tel.: +81-277-30-1458; fax: +81-277-30-1457.
E-mail address: nakagawa@bce.gunma-u.ac.jp (N. Nakagawa).

0378-7753/03/$ – see front matter © 2003 Elsevier Science B.V. All rights reserved.
doi:10.1016/S0378-7753(03)00090-9

2. Experimental

Nafion 112 (DuPont) was used as the electrolyte membrane. In order to activate the proton conductivity, the membrane was pretreated by sequential immersion in boiling solutions of 3 vol.% H_2O_2, de-ionized water, 2.5 mol/dm^3 H_2SO_4, and de-ionized water in that the order for 1 h. The anode catalyst used was Pt (54%)-Ru/C (TEC61E54, Pt/Ru = 1.5, Tanaka Kikinzoku), and was mixed with 5 wt.% Nafion 117 solution (Wako Inc.) and glycerol in the weight ratio of 1:2.5:3, respectively, to prepare a catalyst ink for the anode. A certain amount of the catalyst ink was uniformly painted onto the carbon paper (TGP-H-120, Toray), and it was used as the anode after being dried in a vacuum oven at 353 K for 1 h. Different Pt-Ru loadings were employed for each anode. As the cathode, the Pt/C catalyst layered on the carbon paper with 1.0 mg-Pt/cm^2 was used. In this case, the Pt loading was kept constant at the value for each cathode. The electrolyte membrane was sandwiched between the sheets of the anode and the cathode, and then hot-pressed at 403 K, 10 MPa, for 3 min to assemble the MEA. The electrode area of the MEA was 5 cm^2.

The schematic diagram of the experimental apparatus is shown in Fig. 1. The MEA was set in a single-cell holder (FC05-01SP-REF, ElectroChem Inc.) made of graphite blocks with serpentine flow channels. The holder contained two copper plates outside of the graphite blocks as the current collector. The cell temperature was controlled with heating pads placed outside of the copper plates. The oxidant gas controlled by the flow meter and the pressure regulator was fed to the cathode from the cylinder at atmospheric pressure. The aqueous methanol solution, preheated to a similar temperature as the cell at the inlet, was supplied to the anode using pump (Iwaki, SDK-081).

In the experiment, a liquid-feed DMFC was operated at atmospheric pressure in the temperature range of 303–373 K by feeding aqueous methanol solution to the anode and dry air or dry oxygen to the cathode. A 2 M (=mol/dm^3) methanol solution was fed at 1.5–3.0 ml/min. The open-circuit voltage, current–voltage curve and electrode impedance were measured at each condition by employing an electrochemical measurement system (HAG-5010, Hokuto Denko Co. Ltd.) using the two-terminal method between the anode and cathode.

3. Results and discussion

3.1. Effect of Pt-Ru loading on DMFC performance

Fig. 2 shows the effect of the Pt-Ru loading at the anode on the performance of the DMFC. The current–voltage curve, at the bottom, and the power density curve, at the top, measured for the cells with 1.0–5.7 mg/cm^2 Pt-Ru are shown in the figure. The current density at a high cell voltage increased with the increasing Pt-Ru loading, whereas that at a low cell voltage decreased when the loading was over 3.75 mg/cm^2. This tendency is clearly shown in Fig. 3 where the current densities at 0.4 and 0.05 V were plotted vs. the Pt-Ru loading. The current density at 0.4 V linearly increased with the increased loading and that at 0.05 V reached a maximum when the loading was 3.75 mg/cm^2. At high cell voltages, i.e. low current densities, the activation overvoltage is major portion in the total overvoltage. The increase in the Pt-Ru loading must then reduce the activation overvoltage at the anode. The linear dependence of the increase in current density with the Pt-Ru loading at 0.4 V, shown in Fig. 3, may suggest that the hole in the

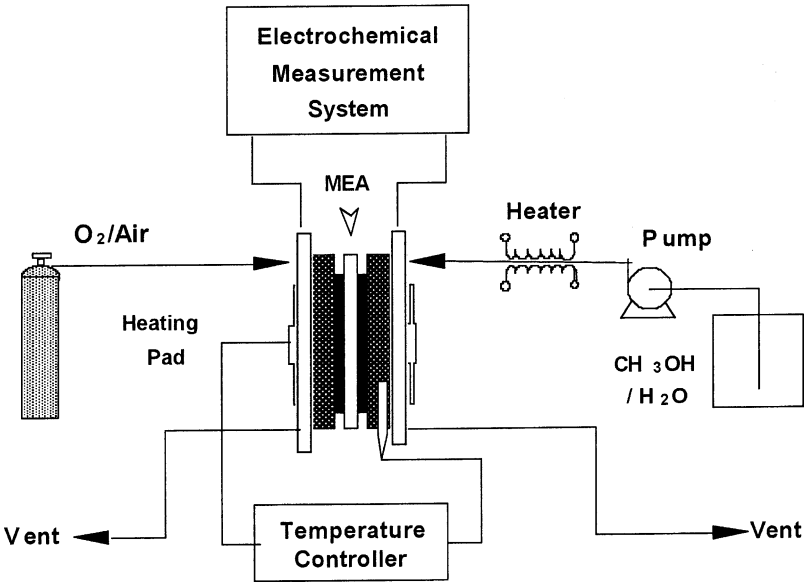

Fig. 1. Schematic diagram of the experimental apparatus.

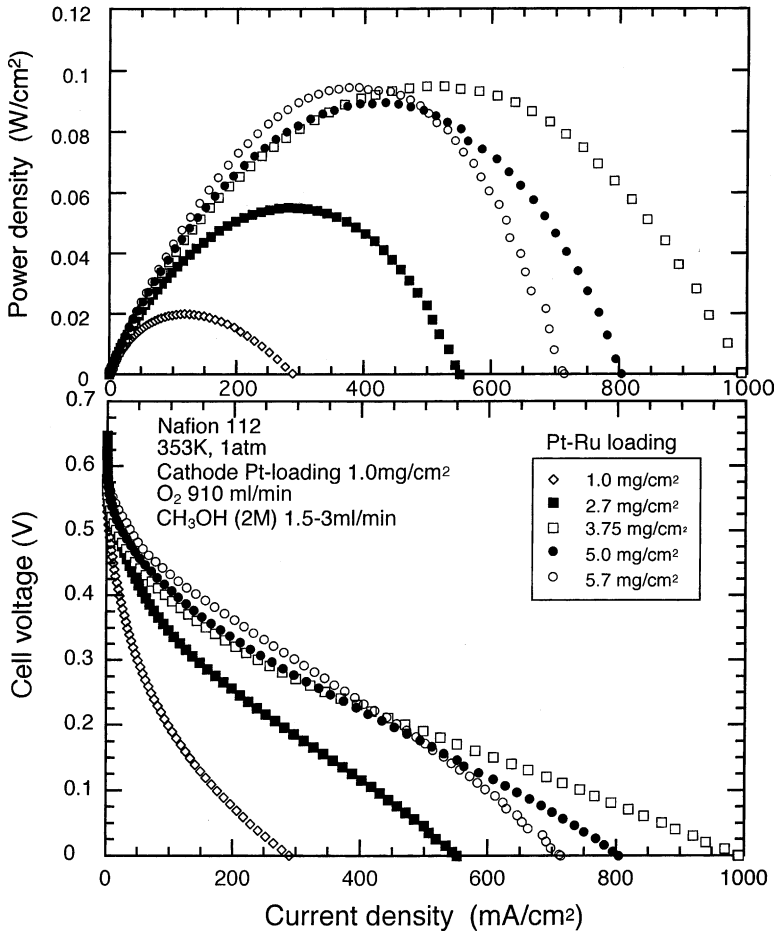

Fig. 2. Effect of Pt-Ru loading at the anode on the DMFC performance at 353 K.

catalyst layer with the Pt-Ru/C effectively functioned as the catalyst for the anode reaction where methanol is decomposed to form H^+ and CO_2. At low cell voltages, i.e. high current densities, abrupt decrease of the cell voltage was shown in the cases where the loading was over 3.75 mg/cm^2 and their curves became sigmoid as shown in Fig. 2. This suggested that the concentration overvoltage significantly increased in these cases. The concentration overvoltage

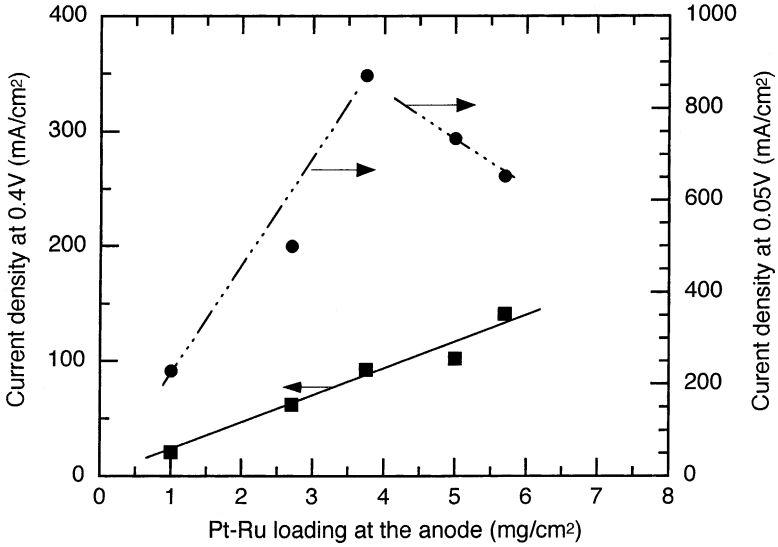

Fig. 3. Relationship between the Pt-Ru loading for the anode and the current densities at high and low cell voltages.

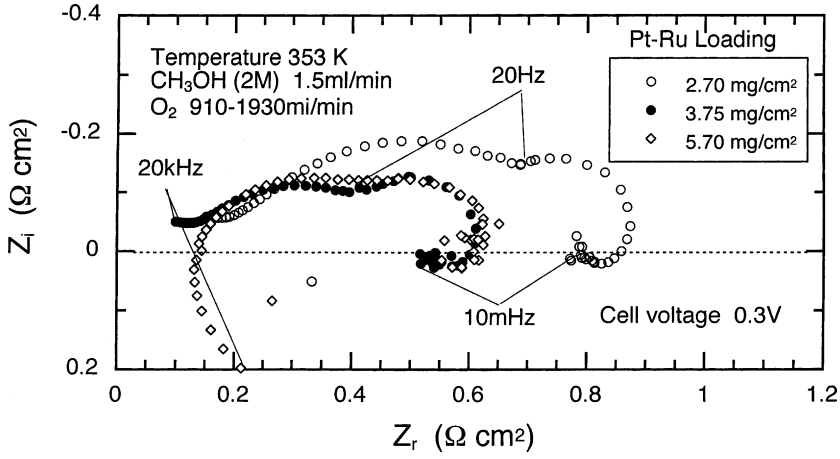

Fig. 4. Electrode impedance plots for DMFC with different Pt-Ru loadings for anode.

resulted from the mass transfer resistance through the catalyst layer. With the increasing Pt-Ru loading, the thickness of the catalyst layer increased because the Pt-Ru loading differed by changing the amount of the Pt-Ru/C catalyst painted on the carbon paper in this experiment. When the methanol concentration was low, abrupt decrease of cell voltage at high current density, similar to that shown in Fig. 2, was also observed in our previous experiment [20]. The decrease in the current density at a low cell voltage when the Pt-Ru loading must result from the concentration overvoltage caused by the mass transfer of methanol through the thicker catalyst layer at the anode.

A comparison of the power density curves shown in the top of Fig. 2 explains that the maximum power density of 0.10 W/cm^2 was obtained from the cell with a 3.75 mg/cm^2 Pt-Ru loading at this condition. A much higher power

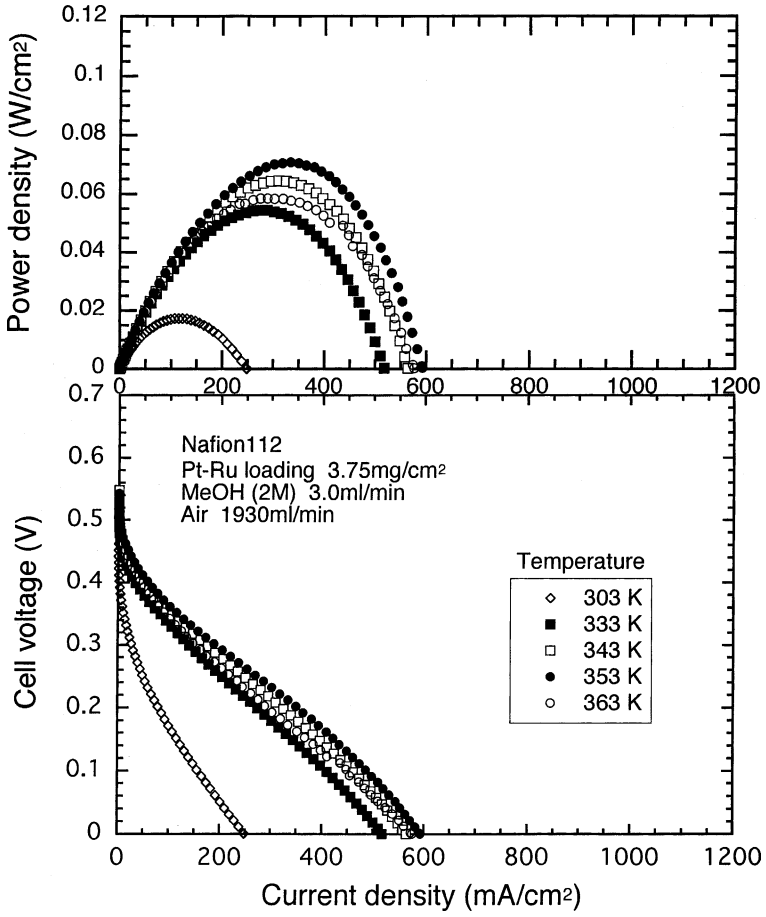

Fig. 5. Effect of temperature on the DMFC performance using air.

density would not be expected even with a much higher Pt-Ru loading if the anode is prepared by a similar procedure using similar materials as in this experiment. For further reduction of the anodic overvoltage, alternate materials or controlling microstructure of the catalyst layer is important. Concentration of PtRu fine particles in the vicinities of the catalyst layer/polymer electrolyte interface or enlargement of the area of reaction sites may be effective to achieve the anodic overvoltage low without increasing the concentration overvoltage.

Fig. 4 shows the impedance plot for the DMFCs with different Pt-Ru loadings measured at a 0.3 V cell voltage. Every plot consisted of double semicircles of which the low frequency side, the right-hand side, includes an inductance loop. The positive values of the imaginary component of the impedance at very high frequency for 5.70 mg/cm^2 may be caused by an unexpected error in the measurement. The inductance loop can be explained by the reaction mechanism with a series of single steps of adsorbed intermediate species with different rates as reported by Muller et al. [18]. The size of the semicircle on the high frequency side, the left-hand side, significantly decreased with the increasing Pt-Ru loading from 2.70 to 3.75 mg/cm^2 and 5.70 mg/cm^2, while that on the low frequency side was almost the same. An electrode reaction generally responds at high frequency compared to the processes with mass transfer. The activation overvoltage attributed to the main factor which controls the current density at the high cell voltage shown in Fig. 2 may be due to electrode reaction at the anode.

3.2. Effect of temperature and oxidant gas

Figs. 5 and 6 show the performance of the DMFC with a 3.75 mg/cm^2 Pt-Ru loading, measured at different temperatures using air and oxygen, respectively. From these figures, the open-circuit voltage was extracted and plotted versus the temperature in Fig. 7. As shown in Figs. 5 and 6, the power density increased with increasing temperature up to 353 and 363 K for air feeding and oxygen feeding, respectively. Over these temperatures, the performance decreased and was unstable. The increase in the temperature increased the open-circuit voltage as shown in Fig. 7 and also reduced the activation overvoltage according to the Arrhenius relation, thus resulting in a higher performance. However, the performance reached a maximum just below the boiling temperature of the solution at 370 K under atmospheric

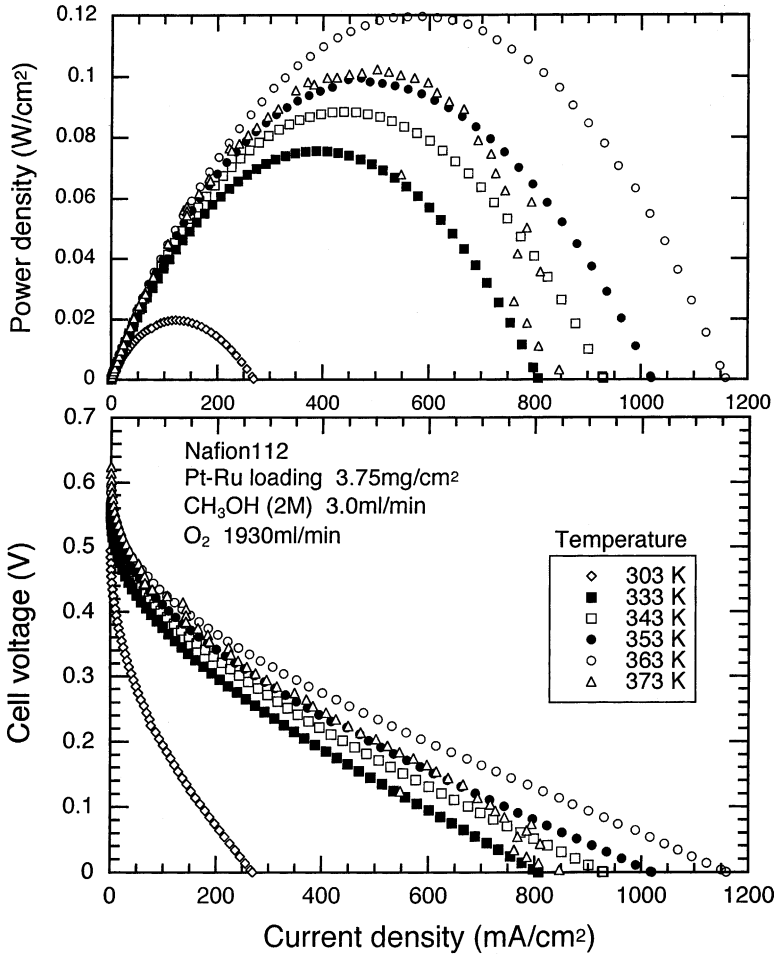

Fig. 6. Effect of temperature on the DMFC performance using oxygen.

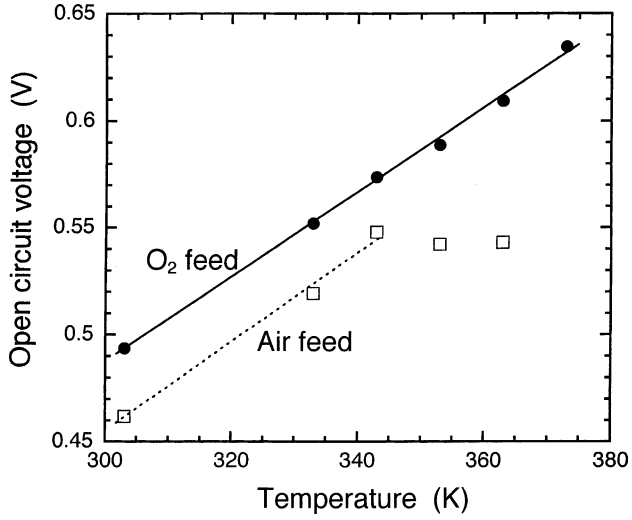

Fig. 7. Effect of temperature on the open-circuit voltages of the DMFCs.

pressure. This suggests that boiling of the solution reduces the cell performance. Small bubbles of the vapor formed in the catalyst layer and diffusion layer may obstruct mass transfer of the liquid methanol.

By comparing Figs. 5 and 6, one can easily understand that the power density with oxygen feeding was almost twice that with air feeding at each temperature except for that of 303 K. This suggests that the overvoltage at the cathode was a relatively large of the total overvoltage of the cell when using air. The maximum power of 0.12 W/cm^2 was obtained at 363 K with oxygen. We may say this is a relatively large value for the power obtained at atmospheric pressure. When using air, the open-circuit voltage (OCV) was lower than that of O_2 feeding, i.e., almost 0.03 V lower below 340 K and 0.05 V or more above 350 K. The decrease in OCV would be caused by the decrease of chemical potential of oxygen that reacts with proton at the cathode. When the circuit was closed, the cell voltage significantly dropped with increasing the current density resulting in sigmoid curves over 333 K. At 303 K, the activation overvoltage was significant and the mass transport was not important thus resulting in similar performance when using air and oxygen.

Figs. 8 and 9 show the electrode impedance plots obtained at different temperatures when using air and oxygen, respectively. The size of the plot decreased with increasing temperature up to 353 and 363 K for air and oxygen feeding, respectively, and the shape of the plot remained similar in

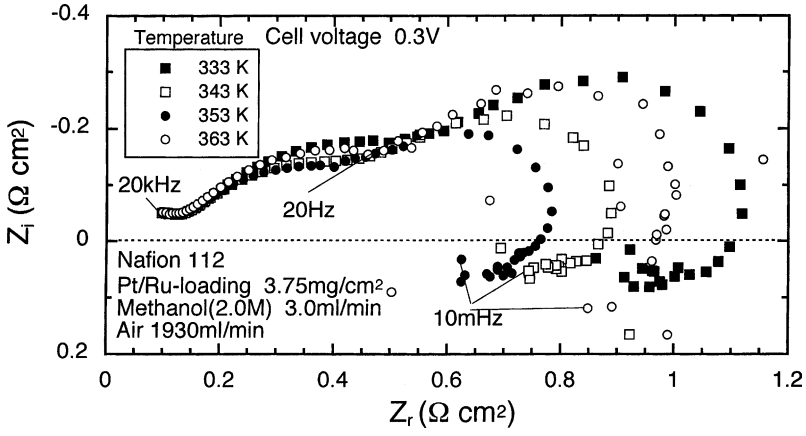

Fig. 8. Electrode impedance plots measured at different temperatures using air.

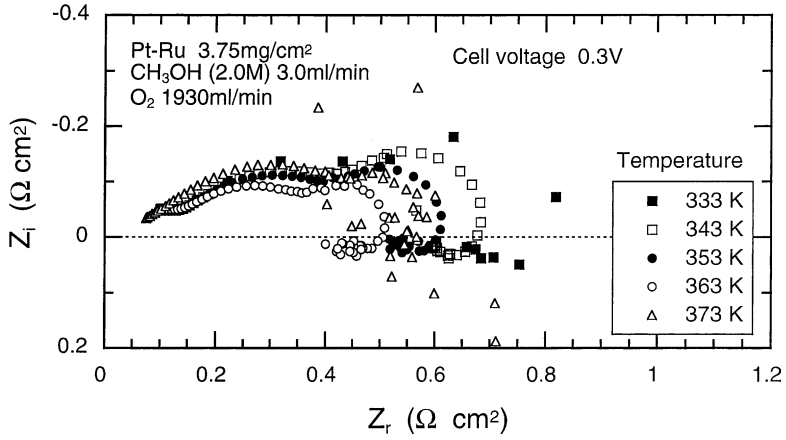

Fig. 9. Electrode impedance plots measured at different temperatures with oxygen feeding.

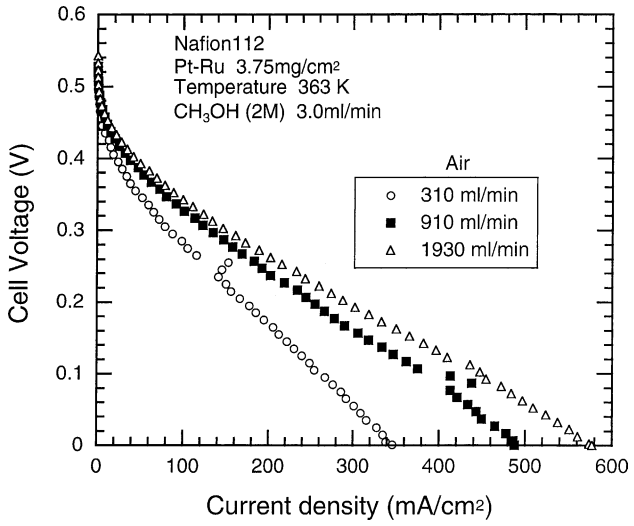

Fig. 10. Effect of flow rate of air to the cathode on the current–voltage curve.

each figure. The size of the semicircle at low frequency for the air feeding was significantly greater than that for the oxygen feeding. This may be related to the mass transfer of oxygen at the cathode because the mass transfer, like gas diffusion and surface diffusion, responds at a relatively low frequency. However, further study is needed to relate the shape of the impedance plot and the reaction mechanism in detail.

3.3. Effect of flow rate of oxidant gas

Figs. 10 and 11 show the effect of flow rate of the air and oxygen on the current–voltage characteristics, respectively. The current–voltage curve was sensitive to the flow rate of air but not to that of oxygen. When the partial pressure of oxygen was low, like air, the mass transfer rate of oxygen from the bulk to the reaction site of the cathode may be affected by the flow rate. An unstable performance that disturbs the current was commonly observed when the flow rate was relatively small in both cases as shown in the figures. That was considered to be due to the effect of produced water that obstructs the mass transfer of oxygen or covers some of the reaction sites at the cathode. These results suggested that the supply of abundant oxygen to the reaction site and smooth removal of the produced water from the electrode was important in order to reduce the overvoltage at the cathode. This is common to the polymer electrolyte fuel cells which use hydrogen as fuel.

Although only the effect of the structure of the anode catalyst layer was evaluated in this paper, further improvements in the cell performance are expected by optimizing the cathode catalyst layer that is planned in our future work.

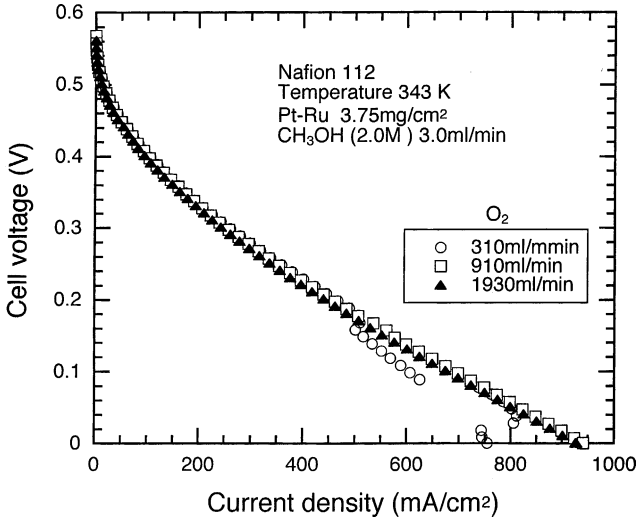

Fig. 11. Current–voltage curves measured at different flow rate of oxygen.

4. Conclusions

A DMFC with different Pt-Ru loadings was prepared and operated at various temperatures and oxidant gas feeding conditions at atmospheric pressure as a fundamental study to investigate the electrode performance of the DMFC. The following conclusions were obtained:

1. The cell performance increased with the increasing Pt-Ru loading for the anode up to a certain amount. Over this amount, the current density at a low cell voltage decreased with its increase, resulting in the reduction of the power density.
2. The cell performance was significantly affected by the oxidant gas, oxygen and air. The feed rate is also important especially for air feeding.
3. The electrode impedance plot shows double semicircles with an inductance loop at low frequency side.
4. A relatively large power density of 0.12 W/cm^2 was obtained at 363 K at atmospheric pressure with optimized Pt-Ru loading for the anode.

Acknowledgements

This work was supported by a Grant-in-Aid for Scientific Research on the priority area of DMFC (grant no. 13134201) from The Ministry of Education, Science, Sports and Culture, Japan. The authors thank Toray Co. Ltd., for providing the carbon paper.

References

[1] C. Lamy, J.M. Leger, S. Srinivasan, in: J.O'M. Bockris, B.E. Conway, R.E. White (Eds.), Direct Methanol Fuel Cells: From a Twentieth Century Electrochemist's Dream to a Twenty-first Century Emerging Technology, Modern Aspects of Electrochemistry, vol. 34, Kluwer Academic Publishers/Plenum Press, Dordrecht/New York, 2001, pp. 53–118.

[2] X. Ren, M.S. Wilsonand, S. Gottesfeld, J. Electrochem. Soc. 143 (1996) L13.
[3] P. Argyropoulos, K. Scott, W.M. Taama, J. Power Sources 79 (1999) 184.
[4] M. Kunimatsu, T. Shudo, Y. Nakajima, JSAE Rev. 23 (2002) 21.
[5] E.S. Steigerwalt, G.A. Deluga, D.E. Cliffel, C.M. Lukehart, J. Phys. Chem. B 105 (2001) 8097.
[6] C. Yang, S. Srinivasan, A.S. Arico, P. Creti, V. Baglio, V. Antonucci, Electrochem. Solid State Lett. 4 (2001) A31.
[7] K. Scott, W.M. Taama, P. Argyropoulos, K. Sundmacher, J. Power Sources 83 (1999) 204.
[8] L.J. Hobson, Y. Nakao, H. Ozu, S. Hayase, J. Power Sources 104 (2002) 79.
[9] S. Hikita, K. Yamane, Y. Nakajima, Jidoushya Gijyutsukai Ronbunsyu 32 (2001) 51.
[10] J.T. Wang, S. Wasmus, R.F. Savinell, J. Electrochem. Soc. 143 (1996) 1233.
[11] X. Ren, T.E. Springer, T.A. Zawodzinski, S. Gottesfeld, J. Electrochem. Soc. 147 (2000) 466.
[12] M. Hogarth, P. Christensen, A. Hamnett, A. Shukla, J. Power Sources 69 (1997) 125.
[13] A.S. Arico, P. Creti, P.L. Antonucci, J. Cho, H. Kim, V. Antonucci, Electrochim. Acta 43 (1998) 3719.
[14] S. Hikita, K. Yamane, Y. Nakajima, JSAE Rev. 23 (2001) 133.
[15] J. Nordlund, A. Roessler, G. Lindbergh, J. Appl. Electrochem. 32 (2002) 259.
[16] K. Scott, P. Argyropoulos, P. Yiannopoulos, W.M. Taama, J. Appl. Electrochem. 31 (2001) 823.
[17] M. Kunimatsu, T. Shudo, Y. Nakajima, Jidoushya Gijyutsukai Ronbunsyu 32 (2001) 81.
[18] J.T. Muller, P.M. Urban, W.F. Holderich, J. Power Sources 84 (1999) 157.
[19] J.T. Mueller, P.M. Urban, J. Power Sources 75 (1998) 139.
[20] Y. Xiu, N. Nakagawa, Kagaku Kogaku Ronbunshu 29 (2003), in press.